Acta Crystallographica Section B
Structural Science
ISSN 0108-7681

Conformational transformation coupled with the order–disorder phase transition in 2-methyl-1,3-cyclohexanedione crystals

Andrzej Katrusiak

Department of Crystal Chemistry, Adam Mickiewicz University, Grunwaldzka 6, 60-780 Poznań, Poland

Correspondence e-mail: katran@amu.edu.pl

Received 1 January 2000
Accepted 17 April 2000

The half-chair conformation of the dynamically disordered molecular ring of 2-methyl-1,3-cyclohexanedione, $C_7H_{10}O_2$, transforms to a sofa below T_c = 244 K, when the crystal undergoes a continuous phase transition induced by the onset of halting large-amplitude vibrations of methylene groups $C(4)H_2$ and $C(5)H_2$. The temperature dependence of the crystal structure has been investigated by X-ray diffraction. The *Ibam* symmetry of the crystal reduces below T_c to space group *Pccn*. The mechanism of the phase transition and of the conversion of the ring conformation is discussed.

1. Introduction

The conformation of molecules or molecular ions is one of their most fundamental characteristics, often responsible for the physical and chemical properties of a substance or for its biological activity. The conformation of a molecule can vary (Eliel & Wilen, 1994; Warshel & Karplus, 1974) and some molecules may exist only when stabilized by vibrational states (Manz *et al.*, 1982; Konarski, 1984). A molecular conformation can be modified by its crystallographic environment, which is occasionally observed for crystals with several symmetry-independent molecules (Katrusiak, 1996; Watenpaugh *et al.*, 1968), for disordered molecules (Rychlewska *et al.*, 1991; Błaszczyk *et al.*, 1996; Katrusiak *et al.*, 1983), polymorphic structures (Głowiak & Sobczak, 1992; Garbauskas *et al.*, 1983; Bernstein, 1979; Bernstein & Hagler, 1978), or for cations forming different salts or different solvates (Thiel *et al.*, 2000). The changes in molecular dimensions (Dunitz, 1995; Braga, 1992), tautomeric forms (Ogawa *et al.*, 1998; Konno *et al.*, 1989), electron transfers (Torrance *et al.*, 1981), polymerization (Yalpani *et al.*, 1983, 1985) *etc.* equally concern the crystals built from small molecules, large biopolymers (Kroon-Batenburg *et al.*, 1986, 1996), isolated molecules (Warshel & Karplus, 1974) or solutions (Lawalle & Zeltman, 1974). In certain cases the crystals may undergo thermodynamic phase transitions which involve transformations of the molecules or ions themselves (Herbstein, 1996; Baudour, 1996; Näther *et al.*, 1996; Richardson *et al.*, 1990; Yang *et al.*, 1989; Byrn *et al.*, 1972; Hazen *et al.*, 1987; Ohashi, 1998).

Conformational transformations are not limited to acyclic moieties, but are also observed for cyclic molecules, which assume different conformations due to a ring inversion (Wysocka *et al.*, 1999) or are partially dynamically or statically disordered. Numerous ring-puckering transformations proceeding continuously within one phase (Molchanov *et al.*, 1986; VanDerveer & Eisenberg, 1974) or coupled with phase transitions were reported (Thuery *et al.*, 1999; Ono *et al.*, 1998; Facey *et al.*, 1996; Katrusiak, 1990; Le Bars-Combe & Lajzerowicz, 1987; Parkinson *et al.*, 1976; Paul & Go, 1969).

The conformational disorder or transformations of molecular fragments, often regarded as a nuisance limiting the accuracy of structural determinations, are immanent features of the molecule affecting its shape, symmetry and properties. Detailed structural information about such transformations can be obtained by diffraction methods. Particularly the studies of the crystals built from small molecules provide insights into the mechanisms of the molecular transformations, which can be then applied to analysing, understanding and predicting the transformations of larger and more complex molecules and systems. Although molecular crystals are sometimes described as oriented gases (Rohleder, 1989), the intermolecular interactions and the couplings of lattice-mode and molecular vibrations cannot be neglected. While large-amplitude vibrations or puckering disorder could not be activated without conformational flexibility in molecules, the interactions with the lattice may stabilize different conformations or exited states of molecules embedded in the crystalline environment (Gdaniec *et al.*, 1999). The mechanisms of coupling between the lattice and molecular modes of vibrations, as well as the role of intermolecular interactions for the crystal and molecular transformations, differ considerably for different substances and are still not fully understood.

Herein we report the conformational transformation and phase transition in 2-methyl-1,3-cyclohexanedione (denoted MCHD). Crystals of MCHD and 1,3-cyclohexanedione (CHD) were reported to undergo structural phase transitions coupled with large-amplitude intramolecular vibrations of the methylene groups in the molecular rings (Katrusiak, 1990, 1991, 1993*a*, 1994). In the crystalline state the molecules of simple β-diketoalkanes are present in the enolized form and are linked into chains by ═O—HO— hydrogen bonds shorter than 2.6 Å (Katrusiak, 1994; Etter *et al.*, 1986; Katrusiak, 1989, 1990; Semmingsen, 1974). A likely conformation of the enolized 1,3-cyclohexanedione ring is a *sofa* with five atoms, C(1), C(2), C(3), C(4) and C(6), forming a planar system and the methylene carbon atom C(5) lying approximately 0.6 Å from this plane. For an isolated molecule two such positions of C(5) on the opposite sides of the molecular ring are energetically equivalent. Each of the $C(5)H_2$ sites is associated with the opposite chirality of the molecules of this compound often used in organic syntheses.

In CHD, above the phase transition at 289 K the methylene group $C(5)H_2$ is dynamically disordered in two symmetry-independent sites. Below 289 K the methylene group becomes ordered in one of these sites. The onset of ordering of $C(5)H_2$ in CHD crystals is accompanied by several structural transformations, such as reorientations of molecules, transfer of the enolic protons in the bistable hydrogen bonds, which is simultaneous with reversing the sequence of the double and single bonds in the alternate π-electron bond system (HO—C═C—C═O transforms into O═C—C═C—OH), or shear shifts of the hydrogen-bonded chains. This first-order phase transition in CHD is marked by a pronounced change of the crystal shape.

The phase transition in MCHD crystals was detected at 244 K and it was postulated that it is induced by the disordering of methylene groups $C(4)H_2$ and $C(5)H_2$ (Katrusiak, 1993*a*,*b*). Several features of the phase transition and of the structure of MCHD crystals are different from those observed for CHD: the phase transition in MCHD appears to have a continuous character, the disordered MCHD molecules lie on mirror planes and the conformation of the cyclohexene ring is a *half-chair* with two disordered methylene groups, $C(4)H_2$ and $C(5)H_2$, at the opposite sides of the molecular plane. As in CHD, the inversion of the $C(4)H_2$ and $C(5)H_2$ methylenes switches the chirality of the enolized MCHD molecule with the relaxation time of 4.0×10^{-9} s at 295 K and 3.4×10^{-8} s at 244 K (Waôsicki *et al.*, 1995).

The present low-temperature structural analysis was primarily undertaken to study the coupling between the molecular transformations and the phase transition of the MCHD crystal.

2. Experimental

Crystals of MCHD were obtained by slow evaporation of its acetone solution at room temperature. They crystallized in the form of colourless elongated prisms. A point-detector KM-4 diffractometer and a KM-4 CCD camera were used, and the crystals were cooled with a stream of gaseous nitrogen from a home-made attachment and an Oxford Cryosystems device, respectively. In the home-made attachment the temperature of the stream was stabilized by an automatic temperature controller within $\pm 0.5^\circ$. Additionally, the crystal temperature was measured independently by a thermocouple placed in the stream 1.0 mm before the sample. Three crystal samples, all rectangular plates, were used for the measurements. The unit-cell dimensions, measured between 118 and 292 K, are listed in Table 1.[1] Below the transition temperature at 244 K the crystal symmetry decreases from space group *Ibam* to *Pccn*, as unequivocally determined from systematic absences: the reflections with odd sums of indices $(h + k + l)$ clearly acquired non-zero intensities. The KM-4 CCD camera was used for collecting the data at 123, 180, 225, 239, 240 and 242 K; the measurements at 240 and 242 K were collected over 2 h each, in the limited reciprocal space of approximately 80% completeness, while complete data sets for the other temperatures were recorded over ~8 h each. Only the intensity data fulfilling the $h + k + l = 2n$ condition were collected with the KM-4 diffractometer at 170, 220, 250 and 293 K. The room-temperature structure (Katrusiak, 1993*b*) served as a starting model for refining the 250 K structure and, after appropriate modifications, for refining the structures of the low-temperature phase. In the refinements of the structural models below T_c the symmetry was reduced to *Pccn* and, in accordance with the convention, the origin of the lattice was shifted by [0.25, 0.25, 0.25]. The C and O atoms were refined with anisotropic thermal parameters. The coordinates of all H atoms and their isotropic temperature factors were refined for

[1] Supplementary data for this paper are available from the IUCr electronic archives (Reference: HR0044). Services for accessing these data are described at the back of the journal.

Table 1
Temperature dependence of the unit-cell dimensions of 2-methyl-1,3-cyclohexanedione.

T (K)	a (Å)	b (Å)	c (Å)	V (Å^3)
118	13.427 (4)	13.689 (7)	6.942 (7)	1276.1
123	13.427 (3)	13.689 (3)	6.946 (2)	1276.7
170	13.426 (5)	13.690 (5)	6.987 (2)	1284.3
198	13.447 (5)	13.686 (4)	7.021 (2)	1292.1
220	13.466 (4)	13.691 (4)	7.053 (2)	1300.3
238	13.487 (4)	13.694 (5)	7.087 (2)	1309.0
242	13.498 (4)	13.691 (4)	7.095 (2)	1311.2
247	13.505 (4)	13.689 (4)	7.111 (3)	1314.5
250	13.510 (3)	13.690 (3)	7.111 (1)	1315.2
253	13.510 (4)	13.689 (4)	7.117 (2)	1316.8
260	13.520 (3)	13.693 (3)	7.132 (2)	1320.4
266	13.524 (4)	13.690 (4)	7.142 (3)	1322.3
293	13.558 (3)	13.696 (3)	7.174 (2)	1332.1

the measurements at 123, 180, 225 and 239 K, however, the temperature factors of the H atoms at one carrier were restrained to one free variable. For the other temperatures the H atoms were recalculated from molecular geometry after each cycle of refinement and their temperature factor was 1.3 or 1.5U_{eq} (for the methyl) of their carriers, except for H(1) for which the coordinates and U_{iso} were free to refine. *SHELXL*93 (Sheldrick, 1993) was used for the calculations. The details of data collections and refinements are listed in Table 2 and the final atomic parameters in Table 3.

3. Results

3.1. Thermal expansion

The temperature dependence of the unit-cell dimensions (Table 1) is plotted in Fig. 1. The thermal expansion of the cell constants or volume are continuous about T_c, within experimental error, which is consistent with the postulated second-order character of this phase transition (Katrusiak, 1993*a*; Waôsicki *et al.*, 1995). Thermal expansion of c significantly increases between 210 and 265 K, while small anomalies appear about T_c in a (a kink) and b (a negative region). The crystal exhibits the largest thermal expansion along [001] and [100], directions perpendicular to the chains of molecules linked by O(1)H$\cdots$O(2^{i}) hydrogen bonds [symmetry code: (i) $1-x, -\frac{1}{2}+y, \frac{1}{2}-z$ in the low-temperature phase, and $\frac{1}{2}-x, -\frac{1}{2}+y, -z$ above T_c; see Fig. 2], while the smallest expansion is along [010], the direction of the chains. This is consistent with the anisotropy of the crystal elasticity (Waôsicki *et al.*, 1995), which results from the anisotropy of intermolecular interactions in the crystal structure, and from the direction of large-amplitude vibrations (LAV) of methylene groups C(4) and C(5), perpendicular to the molecular planes, as shown in Fig. 3. These LAV are reflected in the anisotropy of thermal vibrations of atoms: their thermal ellipsoids are strongly elongated perpendicular to the molecular plane. This concerns all the atoms of the molecule, as the half-chair inversions of the ring require some deformations of the conjugated bond system, and the large-amplitude vibrations of C(4) and C(5) provoke counter-vibrations of the 'rigid' part of the molecule preser-

Table 2
Crystal data and structure refinements for 2-methyl-1,3-cyclohexanedione at 123 and 250 K (low- and high-temperature phases, respectively).

The data for the measurements at 170, 180, 220, 225, 239, 240, 242 and 293 K have been deposited with the Cambridge Crystallographic Data Centre (CCDC), 12 Union Road, Cambridge, England.

Temperature	123 K	250 K
Empirical formula	$C_7H_{10}O_2$	
Formula weight	126.15	
Wavelength (Å)	0.71073	0.71069
Crystal system	Orthorhombic	Orthorhombic
Space group	*Pccn*	*Ibam*
a (Å)	13.427 (3)	13.510 (3)
b (Å)	13.689 (3)	13.690 (3)
c (Å)	6.946 (2)	7.1110 (10)
Volume (Å^3)	1276.7 (5)	1315.2 (5)
Z	8	8
Density (calculated) (Mg m^{-3})	1.313	1.274
Absorption coefficient (mm^{-1})	0.095	0.092
F(000)	544	544
Crystal size (mm)	0.3 × 0.3 × 0.2	0.3 × 0.3 × 0.2
Min./max. θ for data (°)	2.98/29.72	2.12/28.05
Ranges of indices:		
h	−17/16	0/17
k	−18/18	0/18
l	−7/9	0/9
No. of measured reflections	6596	866
No. of independent reflections	1616	866
R_{int}	0.0547	–
Refinement method	Full-matrix least-squares on F^2	Full-matrix least-squares on F^2
Data/parameters	1616/117	866/104
Goodness-of-fit on F^2	1.104	1.027
Final R_1/wR_2 indices [$I \geq 2\sigma_I$]	0.0531/0.1439	0.0447/0.1307
R_1/wR_2 indices (all data)	0.0673/0.1565	0.0666/0.1379
Max. diff. peak/hole (e Å^{-3})	0.437/−0.311	0.250/−0.182

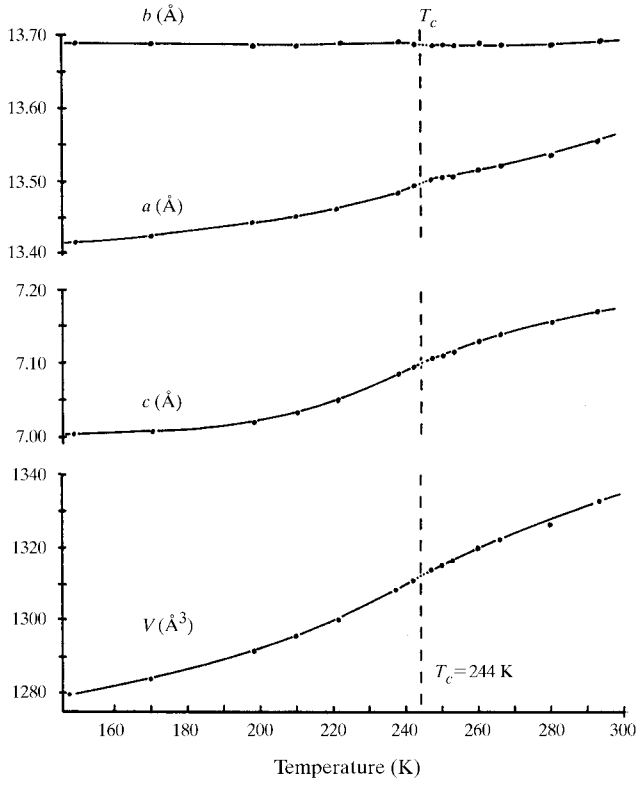

Figure 1
Temperature dependence of the unit-cell dimensions of MCHD. The dotted lines about T_c = 244 K serve only as a guide to the eye.

Table 3
Atomic coordinates ($\times 10^4$) and equivalent [isotropic for H(1)] temperature parameters (Å^2 $\times 10^3$) for 2-methyl-1,3-cyclohexanedione at 123 and 250 K (see Table 2).

U_{eq} is defined as one third of the trace of the orthogonalized U_{ij} tensor.

	x	y	z	U_{eq}
123 K				
O1	0.56748 (7)	0.45070 (6)	0.23059 (14)	0.0204 (3)
H1	0.5274 (18)	0.3894 (17)	0.229 (3)	0.046 (7)
O2	0.52702 (8)	0.78702 (7)	0.2790 (2)	0.0248 (3)
C1	0.50884 (10)	0.52910 (9)	0.2458 (2)	0.0155 (3)
C2	0.55143 (10)	0.61931 (9)	0.2478 (2)	0.0165 (3)
C7	0.66143 (10)	0.63485 (10)	0.2226 (2)	0.0253 (4)
C3	0.48991 (10)	0.70373 (9)	0.2796 (2)	0.0175 (3)
C4	0.37998 (9)	0.68976 (9)	0.3210 (2)	0.0205 (3)
C5	0.33758 (9)	0.60178 (9)	0.2154 (2)	0.0195 (3)
C6	0.39853 (10)	0.51077 (9)	0.2618 (2)	0.0181 (3)
250 K				
O1	0.31902 (8)	0.20153 (8)	0	0.0524 (4)
H1	0.283 (2)	0.140 (2)	0	0.086 (9)
O2	0.27336 (11)	0.53660 (9)	0	0.0710 (6)
C1	0.25946 (11)	0.27924 (10)	0	0.0380 (4)
C2	0.30069 (10)	0.36961 (10)	0	0.0396 (4)
C7	0.40993 (13)	0.38555 (14)	0	0.0595 (7)
C3	0.23808 (13)	0.45325 (11)	0	0.0522 (5)
C4	0.1283 (2)	0.4382 (2)	−0.0525 (4)	0.0523 (11)
C5	0.0904 (2)	0.3484 (2)	0.0489 (5)	0.056 (2)
C6	0.15042 (12)	0.25947 (12)	0	0.0465 (5)

ving the angular momentum of the molecule. The continuous character of the phase transition can also be observed from the intensities of reflections systematically absent in the high-temperature phase. Fig. 4 shows that the ratio of sums of reflections with $(h + k + l)$ odd divided by the sum of all measured reflections increases continuously on cooling MCHD below T_c, and still saturates slowly below 123 K.

3.2. Ring conformation

The expected conformation for a 2,3-cyclohexenone ring, containing three adjacent Csp^2 and three Csp^3 atoms, is *sofa* (Etter *et al.*, 1986). The *sofa* conformation was observed in three polymorphic crystals of CHD and an inclusion compound of CHD with benzene (Etter *et al.*, 1986; Katrusiak, 1991, 1992). Meanwhile, the dynamically disordered ring of MCHD adopts a *half-chair* conformation. A similar *half-chair* conformation was recently observed in the disordered ring of 3-oxo-1-cyclohexene-1-carboxylic acid (Barcon *et al.*, 1998). It was postulated that the unexpected half-chair conformation in MCHD may result from the different magnitudes of the moments of inertia between MCHD and CHD: in the CHD molecule the smallest of the diagonal components of the inertia tensor corresponds to the direction parallel to C(1)···C(3), while the methyl substituent at C(2) considerably increases this value (Katrusiak, 1994). It is also plausible that in the crystalline state the half-chair conformation of the ring may be stabilized by intermolecular interactions with neighbouring molecules. In the half-chair conformation C(5) and its H atoms are located much closer to the plane of the molecule than for the sofa conformation. In MCHD the vibrations of C(5) are limited from both sides of the molecular plane by interactions with neighbouring chains. At 293 K the intermolecular distance between half-occupied sites of H(51) and O(1^{ii}) is 2.56 Å [symmetry code: (ii) $\frac{1}{2} - x, \frac{1}{2} - y, \frac{1}{2} - z$], when C(5) is deflected 0.380 (3) Å from the molecular plane. A sofa conformation of the ring would require that C(5) moved by more than 0.6 Å off the molecular plane and then H(51)···O(1^{ii}) would be considerably shorter than the sum of van der Waals radii of H and O. The role of the interchain contact H(51)···O(1^{ii}) for the conformation of the ring, and the mode of the large-amplitude intramolecular vibrations, is further corroborated by a correlation between the thermal contraction of c and the changes in the deflection of C(5) from the molecular plane (Table 4) in the high-temperature phase: between 293 and 250 K the interplanar distance (c/2) contracts by 0.031 (2) Å and the deflection of C(5) decreases by 0.032 (4) Å. Fig. 5 shows the displacements of atoms C(4) and

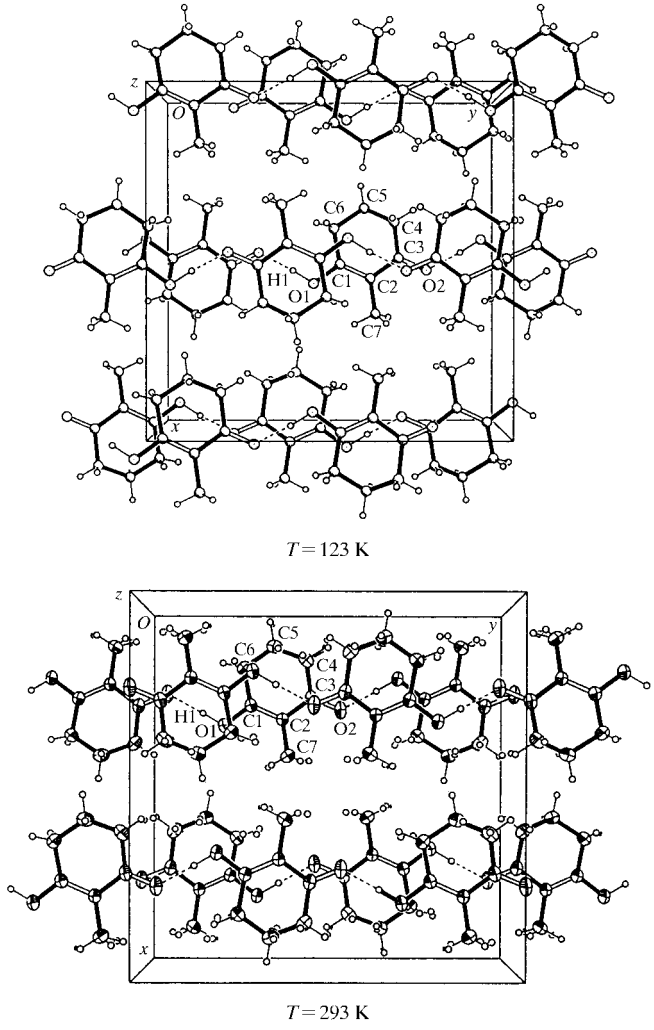

Figure 2
Two layers of hydrogen-bonded molecules: (*a*) in the low-temperature structure at 123 K and (*b*) the *ORTEP* (Johnson, 1965) drawing of the high-temperature structure at 250 K, both viewed down [001]. The thermal ellipsoids are drawn at the 50% probability level. Part (*b*) only shows one conformation of the disordered cyclohexane rings, for clarity. The H atoms are represented as small circles of arbitrary radius. The double bonds are shown as double lines and the hydrogen bonds as dashed lines.

Table 4
Bond lengths (Å) and angles (°) for 2-methyl-1,3-cyclohexanedione at 123 and 250 K (see Table 2 and CCDC for other temperatures).

Temperature	123 K	250 K
O(1)—C(1)	1.335 (2)	1.334 (2)
O(2)—C(3)	1.244 (2)	1.237 (2)
C(1)—C(2)	1.361 (2)	1.357 (2)
C(1)—C(6)	1.506 (2)	1.498 (2)
C(2)—C(3)	1.438 (2)	1.424 (2)
C(2)—C(7)	1.502 (2)	1.492 (2)
C(3)—C(4)	1.516 (2)	1.544 (3)
C(4)—C(5)	1.521 (2)	1.514 (4)
C(5)—C(6)	1.525 (2)	1.504 (3)
O(1)—C(1)—C(2)	118.84 (12)	118.66 (14)
O(1)—C(1)—C(6)	116.85 (11)	116.69 (13)
C(2)—C(1)—C(6)	124.30 (12)	124.65 (13)
C(1)—C(2)—C(3)	119.31 (12)	119.30 (13)
C(1)—C(2)—C(7)	122.71 (12)	122.65 (14)
C(3)—C(2)—C(7)	117.96 (11)	118.05 (14)
O(2)—C(3)—C(2)	120.40 (12)	120.9 (2)
O(2)—C(3)—C(4)	120.41 (11)	119.6 (2)
C(2)—C(3)—C(4)	119.16 (10)	117.64 (14)
C(3)—C(4)—C(5)	111.90 (11)	108.5 (2)
C(4)—C(5)—C(6)	110.11 (11)	111.4 (2)
C(1)—C(6)—C(5)	112.08 (10)	112.58 (14)

C(5) from the least-squares plane fitted to the other non-H atoms of the molecule. It is apparent that above T_c the disordered molecular ring is present in the half-chair conformation and that below T_c it transforms to a sofa, which becomes slightly less and less distorted on lowering the temperature. At 250 K the C(4) atom becomes even more distant from the molecular plane than C(5). It is plausible that the flattened conformation of the ring in the range of a few degrees below T_c is due to the large-amplitude vibrations of C(5) in the strongly asymmetric potential energy well. Such vibrations also would reduce d[C(4)], as observed in Fig. 5, and would affect the inclination of the molecule in the crystal lattice. A clearly anomalous change in the inclination of the molecular plane is observed below T_c, which apparently accommodates the elevation of C(5) and minimizes its interactions with the crystal surrounding, as illustrated in Fig. 6. Fig. 7 shows the molecular tilt and the shortest contacts of C(5), with O atoms O(1^{ii}) and O(1^{iii}) (symmetry codes are given in the caption of Fig. 7), to the molecules of the neighbouring chains along [001] and [100], respectively. This difference further increases at still lower temperatures. On approaching T_c in the low-temperature phase both contacts C(5)···O(1^{ii}) and C(5)···O(1^{iii}) become longer, and above T_c they shorten by ∼0.05 Å. This could indicate that the inter-

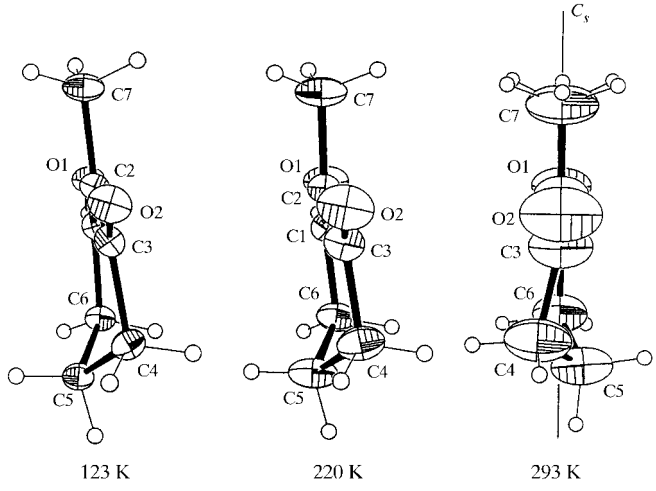

Figure 3
2-Methyl-1,3-cyclohexanedione molecule at 123, 220 and 293 K viewed along [010] in the crystal. In the drawing of the molecule at 293 K only one set of disordered methylene groups, C(4) and C(5), have been indicated for clarity, while the other set can be generated by the (vertical) mirror plane C_s comprising all the other non-H atoms of the molecule; this drawing also shows the disorder of methyl C(7)H_3, for which clearly two sets of H positions with half occupancies have been found in ΔF maps.

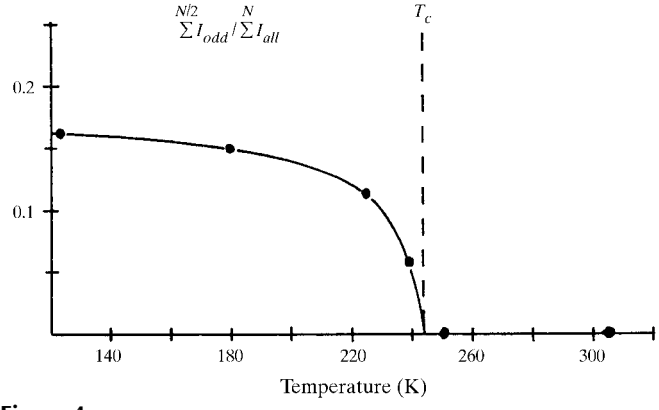

Figure 4
The temperature dependence of the ratio $\sum^{N/2} I_{\rm odd} / \sum^{N} I_{\rm all}$, where $\sum^{N/2} I_{\rm odd}$ is the sum of the intensities of reflections extinguished by the Bravais cell I, for which sums of Miller indices $h + k + l$ are odd, and $\sum^{N} I_{\rm all}$ is the sum of all measured intensities. The sums include negative intensities to avoid zero-intensity bias and only full data sets, measured at 123, 180, 225 and 235 K, have been used. The values obtained are: 0.16215 (7), 0.15074 (13), 0.11330 (8) and 0.05861 (4), respectively; the standard deviations have been calculated by the method of total differential basing on the counting statistics of the intensity measurements.

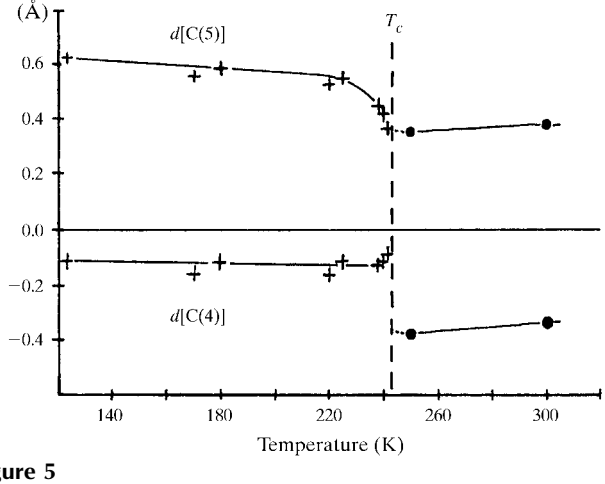

Figure 5
Temperature dependence of the distances of atoms C(4) and C(5) to the least-squares plane fitted to the other non-H atoms of the molecule. The dashed vertical line marks T_c at 244 K. The thin and dotted lines are drawn as a guide to the eye.

molecular interactions of C(5) are not the primary cause of the transformation of the ring conformation to half-chair above T_c. On the other hand, the lengthening of contacts C(5)···O(1^{ii}) and C(5)···O(1^{iii}) immediately below T_c may be due to the asymmetric shape of the potential energy function on approaching the height of the energy barrier. As illustrated in Fig. 8, this asymmetry would shift the center of the density of the vibrating atom C(5) closer to the plane of the ring, and hence further from O(1^{ii}) and O(1^{iii}). The intensifying intermolecular interactions of C(5)H_2 would have a similar effect, however, it should not concern C(4)H_2 as it has longer intermolecular contacts. As shown in Fig. 5, the centre of C(4) also moves closer to the ring plane immediately below T_c, but this effect is considerably smaller than for C(5).

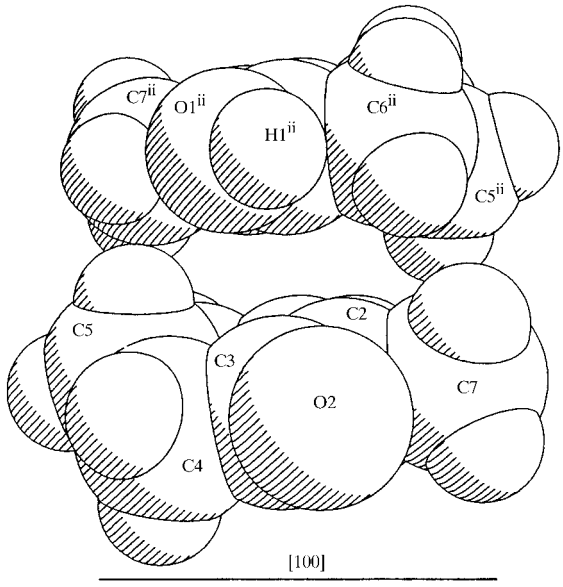

Figure 6
Two MCHD molecules of neighbouring chains at 123 K represented as space-filled models, viewed down the [010] direction of the chains. The pairs of molecules have two close contacts between their methylene C(5)H_2 and hydroxyl O(1) atoms. The horizontal line at the bottom was drawn parallel to [100] to visualize the tilts of the molecules. Symmetry code: (ii) $1-x, 1-y, -z$.

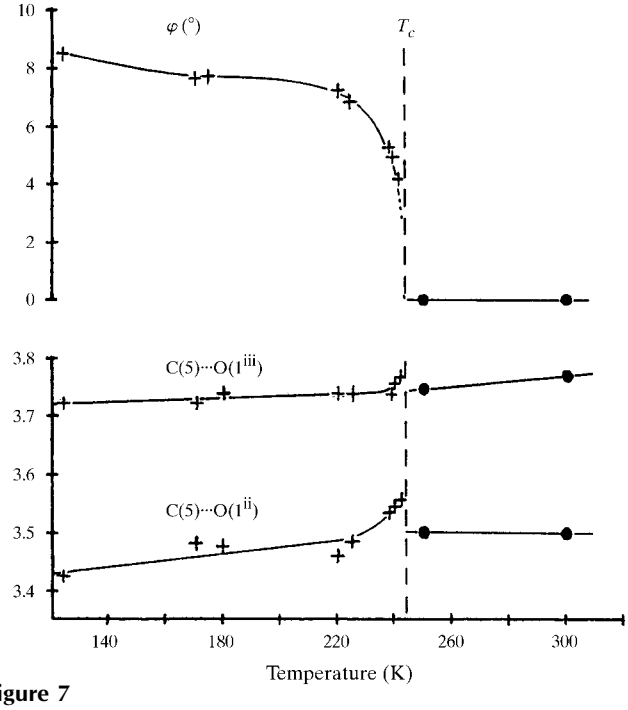

Figure 7
The inclination angle between the least-squares plane fitted to atoms O(1), O(2), C(1)–(6) and crystal plane (001), φ; and the temperature dependence of the closest interchain contacts of atom C(5): to O atoms O(1^{ii}) and O(1^{iii}). The symmetry codes are: (ii) $1-x, 1-y, -z$ and (iii) $\frac{1}{2}+x, 1-y, \frac{1}{2}-z$ for the low-temperature phase below 244 K; (ii) $\frac{1}{2}-x, \frac{1}{2}-y, \frac{1}{2}-z$ and (iii) $\frac{1}{2}+x, \frac{1}{2}-y, -z$ for the high-temperature phase above T_c. The thin and dotted lines are drawn as a guide to the eye.

3.3. Hydrogen bonding and the H site

Hydrogen bonds play a central role in the structural transformations which follow the halting of the LAV of the methylene C(5) atom in CHD at 286 K (Katrusiak, 1990, 1991, 1992). In the MCHD structure the dimensions of the O(1)H···O(2^{i}) hydrogen bond change continuously with temperature, as shown in Fig. 9. Between 123 and 225 K the O(1)···O(2) distance insignificantly increases and a more significant increase is observed above T_c. It appears that about T_c the temperature dependencies of Donohue angles C(1)—O(1)···O(2′) (denoted η'_d) and O(1)···O(2′)═C(2′) (η'_a) smoothly change from convex to concave, and *vice versa*, respectively. The angles describe the mutual orientation of the hydrogen-bonded molecules (Katrusiak, 1995*a*). Values of η'_d and η'_a depend on the hybridization of the O atoms, coupled to the site of the proton in the hydrogen bond (Katrusiak, 1992, 1993*c*, 1998). Below T_c the angle η'_a somewhat decreases and η'_d increases its value. These changes are reflected in the

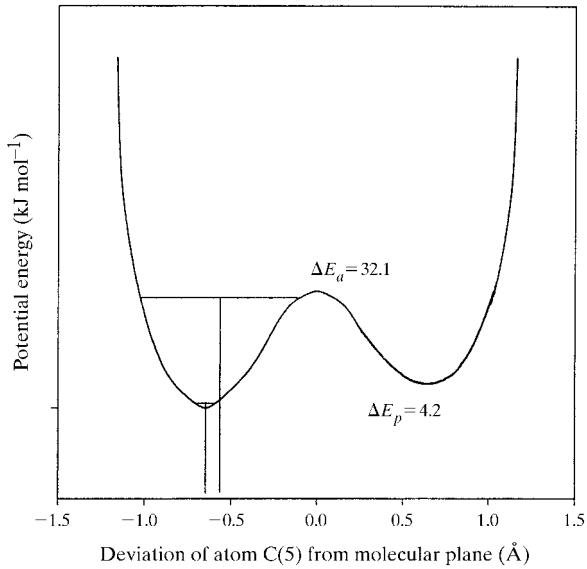

Figure 8
Double-well potential-energy function of C(5) in the 2-methyl-1,3-cyclohexanedione ring below T_c, with indicated centres of two energy levels, one close to the bottom and the other close to the top of the barrier. The energy of activation ΔE_a and the difference between the minima ΔE_p were obtained from NMR studies by Waôsicki *et al.* (1995). E_a changes to 26.1 kJ mol^{-1} above 244 K.

Table 5
Hydrogen-bond dimensions in 2-methyl-1,3-cyclohexanedione at varied temperatures.

The angle ρ between the line passing through O(1) and O(2) of one molecule and the [010] direction describes the inclination of the molecules to the direction of the chains. Also the deviations of methylene atoms C(4) and C(5) from the least-squares plane fitted to the remaining non-H atoms of the molecule, denoted d[C(4)] and d[C(5)] respectively, have been given. The negative sign of d[C(5)] indicates the location of C(5) on the opposite site of the plane to C(4).

	123 K	170 K	180 K	220 K	225 K	239 K	250 K	293 K
O(1)···O(2^{i})	2.576 (1)	2.577 (4)	2.578 (3)	2.578 (2)	2.579 (3)	2.576 (3)	2.580 (2)	2.588 (2)
O(1)—H(1)	1.00 (2)	0.99 (3)	1.13 (4)	1.00 (3)	1.05 (5)	0.98 (5)	0.97 (3)	0.93 (3)
H(1)···O(2^{i})	1.58 (2)	1.60 (3)	1.45 (4)	1.59 (3)	1.53 (5)	1.60 (5)	1.61 (3)	1.66 (3)
O(1)—H(1)···O(2^{i})	175 (2)	166 (5)	177 (3)	168 (4)	175 (4)	176 (3)	178 (3)	175 (3)
C(1)—O(1)—H(1) (η_d)	111.1 (13)	110.4 (18)	115 (2)	111.2 (16)	117 (3)	113 (3)	112.7 (18)	110.3 (19)
H(1)···O(2^{i})═C(3^{i}) (η_a)	128.8 (8)	129.4 (9)	126 (2)	129.3 (10)	126 (2)	128.6 (18)	129.2 (11)	130.6 (12)
C(1)—O(1)···O(2^{i}) (η'_d)	114.25 (8)	114.4 (2)	114.49 (16)	114.25 (14)	114.37 (15)	114.2 (2)	113.97 (10)	113.63 (11)
O(1)—O(2^{i})═C(3^{i}) (η'_a)	126.86 (9)	127.20 (13)	127.42 (17)	127.76 (13)	127.82	128.2 (2)	128.40 (12)	128.75 (14)
ρ	7.90 (2)	7.7 (4)	7.94 (4)	8.1 (3)	7.98 (4)	7.90 (4)	7.66 (9)	7.96 (3)
d[C(4)] (Å)	0.114 (2)	0.159 (9)	0.125 (5)	0.160 (21)	0.118 (5)	0.126 (7)	0.373 (3)	0.339 (4)
d[C(5)] (Å)	−0.614 (2)	−0.556 (8)	−0.586 (6)	−0.529 (30)	−0.547 (7)	−0.449 (8)	−0.348 (3)	−0.381 (3)

Symmetry codes: (i) $1-x, y-\frac{1}{2}, \frac{1}{2}-z$ for 123–239 K; $\frac{1}{2}-x, y-\frac{1}{2}, z$ for 250–293 K.

orientation of the molecules, which are tilted to accommodate the difference between η'_d and η'_a. Thus, the difference ($\eta'_a - \eta'_d$) can be related to the tilt of the molecules, ρ (see Table 5).

The likelihood of enolic proton transfer in the hydrogen bond between chemically equivalent groups is connected with the value of the angle ρ, as such a transfer requires that the molecules rotate to change their tilt to $-\rho$ (Katrusiak, 1992, 1994). Hence, the difference ($\eta'_a - \eta'_d$) and tilt ρ can be used as a measure of the contribution of the crystal field towards stabilization of the H atom at its site. In the pseudosymmetric crystal structures, for example, KDP-type ferroelectrics (KDP denotes KH_2PO_4), the temperature of the proton (deuteron) disordering can be correlated with ρ (Katrusiak, 1995*b*). It was established by solid-state ^{1}H NMR second-moment measurements that in the CHD structure stochastic proton transfers, coupled with molecular reorientations, are present in the high-temperature phase above 286 K, where ρ = 3.38 (2)°, but also in the low-temperature phase where the crystal is cooled down to ∼190 K (Pajaôk *et al.*, 1992). In the low-temperature phase of the CHD angle ρ is ∼7.2°, thus the amplitudes of the molecular reorientations are larger than above 286 K. Such stochastic or soliton-like rearrangements of crystal structures cannot be detected in routine X-ray measurements (Katrusiak, 1994). The second-moment NMR study of MCHD could not detect hydrogen transfers coupled with molecular reorientations in this structure (Waôsicki *et al.*, 1995). This is consistent with the structural results, as the hydrogen bond and its environment in MCHD are not pseudosymmetric (Katrusiak, 1992), and the angle ρ in MCHD is 7.96 (3)° at 293 K, thus considerably larger than the ρ angle in the KDP-type ferroelectrics (Katrusiak, 1995*b*) or in the high-temperature CHD phase. On cooling the MCHD structure, ρ decreases to 7.66 (9)° at 250 K, differently than in most OH---O bonded structures where the tilt of the molecules increased at lower temperatures does not change at T_c and then increases slowly on lowering the temperature (Table 5).

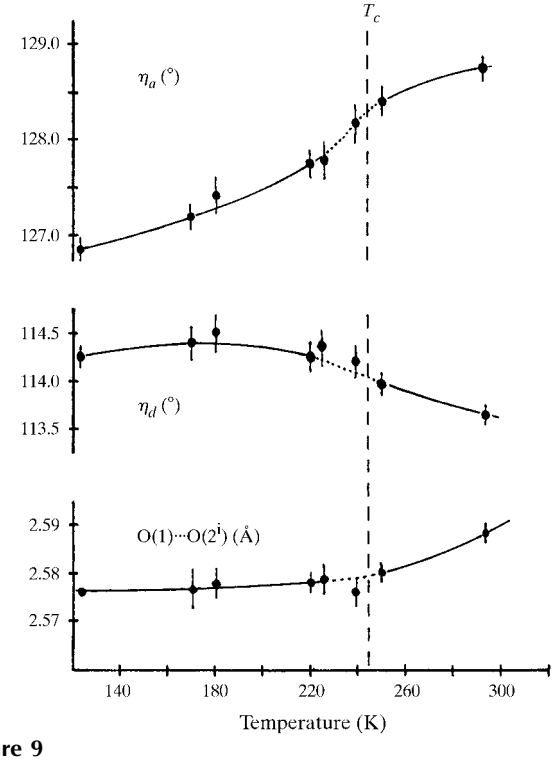

Figure 9
The temperature dependence of the O(1)H···O(2^{i}) hydrogen-bond dimensions: O(1)···O(2^{i}) distance and η'_d and η'_a Donohue angles (see the text). The thin lines are guides to the eye.

4. Discussion

Several structural contributions, both intramolecular and intermolecular, to the phase transition of the MCHD crystals can be identified.

In the low-temperature phase the molecules are present in the slightly distorted sofa conformation. This distortion of the energetically favoured sofa towards a half-chair may reflect the influence of the crystal environment in deforming the molecule: the short contact C(5)···O(1^{ii}) 'squeezes' the molecular ring. This effect of the environment is minimized when the molecule is tilted with respect to the plane (001) (see Figs. 3, 5 and 6) and by the ring distorting towards half-chair.

As the temperature increases towards T_c, the larger amplitudes of thermal vibrations intensify the interactions of C(5) with neighbouring O(1^{ii}). This is reflected in the C(5)$\cdots$O(1^{ii}) distance steadily increasing until ~225 K, above which it rises sharply until T_c. In terms of structural transformations the elongation of C(5)$\cdots$O(1^{ii}) is partly due to the thermal expansion of c (Fig. 1), but mainly due to the increased ring distortion towards half-chair (Fig. 4) and to the ring flattening because of the increasingly asymmetric potential function close to T_c (Fig. 8).

The C(5)$\cdots$O(1^{iii}) distance is considerably longer than C(5)$\cdots$O(1^{ii}) and these two contacts are approximately perpendicular: the direction of C(5)$\cdots$O(1^{ii}) is almost parallel to [001], while C(5)$\cdots$O(1^{iii}) is almost parallel to [100]. A similar temperature dependence of these contacts (Fig. 7) may result from intermolecular interactions and from the conformational properties of the molecule itself. A slower rise of the C(5)$\cdots$O(1^{ii}) distance above T_c (Fig. 7) may mean that the vibrations of C(5) become coupled with the lattice mode vibrations and that the movements of the atoms and molecules along [001] become correlated. It should be noted that the ellipsoids of anisotropic thermal vibrations of the atoms are clearly elongated along [001] and at 220 K their amplitudes are ~0.25 Å for C(4), C(5) and O(1). At this temperature the contacts of methylene H atoms of 2.65 and 2.78 Å for H(5A)$\cdots$O(1^{ii}) and H(5B)$\cdots$O(1^{iii}), respectively, are somewhat longer than the sum of the van der Waals radii of H and O, however, thermal vibrations of these atoms intensify their interactions. It is plausible that at 244 K the structure cannot accommodate the increasing C(5)$\cdots$O(1^{ii}) interactions, unless the vibrations of the neighbouring molecules become coupled and the molecules change their conformation.

Above T_c the ring conformation changes to half-chair (Fig. 5), methylenes C(4)H$_2$ and C(5)H$_2$ become disordered, the time-average molecular plane aligns along (001) (Figs. 3 and 7) and the symmetry of the crystal increases from *Pccn* to *Ibam*. Between 220 and 243 K the amplitudes of thermal vibrations of C(4), C(5) and O(1) along [001] increase from 0.25 to 0.30 Å, which correlates with the increased C(5)$\cdots$O(1^{ii}) distance (Fig. 7). This distance remains almost constant above T_c, despite increased amplitudes of the atomic vibrations to ~0.35 Å along [001] at 293 K.

It is apparent that the potential energy of the molecule is different for the sofa and half-chair conformations (see Fig. 10). The potentials for the ring-puckering vibrations in these conformations are different and are affected differently by the crystal field. The energy of the crystal cohesion forces can be assessed from the 'static' data of van der Waals contacts, as discussed above, however, the kinetic energies of the molecular and lattice vibrations are more difficult to evaluate from structural data. The large-amplitude vibrations in the half-chair conformation may be strongly coupled with the electronic structure of the MCHD molecule, as they involve some deformations of the C(3)=O(2) π-electron region. The ring-puckering vibrations are highly anharmonic, however, to estimate the energy of the vibrations an approximation of the harmonic oscillator, for which the potential and kinetic energies are equipartitioned, can be applied. In this approximation the mean energy of the vibrating molecule built of N atoms, $\langle E\rangle$, is

$$\langle E\rangle = \tfrac{1}{2}\sum_{i=1}^{N} M_i\omega_i^2 A_i^2, \qquad (1)$$

where M_i is the mass of the ith atom vibrating with frequency ω_i and amplitude A_i.

The principle of conservation of the angular momentum requires that for the sofa conformation all the other atoms vibrate in response to the vibrations of C(5) about the axis perpendicular to the bonds C(1)—C(6) and C(3)—C(4), while for the half-chair conformation about the axis perpendicular to the bonds C(1)=C(2) and C(4)—C(5). By further assuming that the energy of vibrations of the other atoms is proportional to the energy of vibrations of C(5)H$_2$ for the sofa, and of C(4)H$_2$ and C(5)H$_2$ for the half-chair, that the frequencies of the vibrations are all equal, that vibrations of C(4) and C(5) are independent and by neglecting all the vibrations other than those along [001], comparison of the energies of the vibrations for the sofa, E_s, and half-chair, E_h, conformations is reduced to the ratio of the squared amplitudes of the vibrating methylene groups

$$\langle E_h\rangle/\langle E_s\rangle = \left[A_{4s}^2 + A_{5s}^2\right]/A_{5h}^2, \qquad (2)$$

where indices s and h denote the amplitudes for the modes of ring vibrations in the sofa and half-chair conformations, respectively. This very rough approximation gives the energy of ring puckering vibrations of the sofa 50% higher than for the half-chair. The lower $\langle E_h\rangle$ energy is consistent with the lower temperature of the phase transition for MCHD (244 K) compared with CHD (286 K). It would also contribute to the explanation of the transformation of the molecular conformation of the MCHD ring from sofa in the low temperature phase to half-chair above T_c.

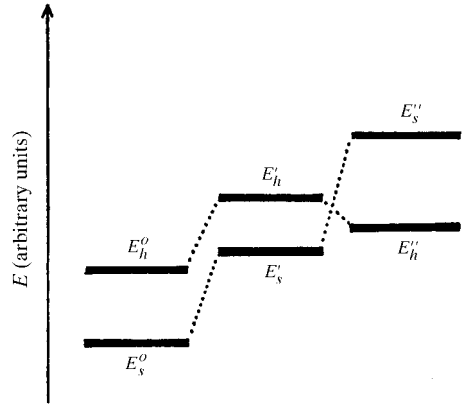

Figure 10
Schematic representation of the potential and kinetic energy components of a molecule in sofa and half-chair conformations, for the isolated molecule, and the molecule embedded in a crystal environment. E^o denotes the potential energy of the molecule in the sofa and half-chair conformations at 0 K, E' denotes the energies increased by the ring-puckering vibrations, *i.e.* $E_s' = E_s^\circ + \langle E_s\rangle$ [see equations (1) and (2)], and E'' includes the interaction energies in the crystal lattice; subscripts s and h refer to the sofa and half-chair conformations, respectively.

Despite the abrupt freezing of the vibrations of $C(4)H_2$ and $C(5)H_2$ at T_c and the discontinuous transformation of the ring conformation (Fig. 5), the phase transition in MCHD is continuous, as confirmed by the temperature dependence of the unit-cell dimensions (Fig. 1), DTA (differential thermal analysis; Katrusiak, 1993*a*), DSC (differential scanning calorimetry), Brillouin scattering and dielectric measurements (Waôsicki *et al.*, 1995). Thus, the microstructural transformations of the ring conformation (Fig. 5), molecular tilt φ and intermolecular contacts (Fig. 7), or the changes in hydrogen-bond dimensions and Donohue angles (Fig. 9), compensate for and accommodate lattice strains. It appears that only these structural transformations, which are directly coupled to the ring inversions, can be described by double-well potentials.

The order parameter of the transition can be connected with the angle of molecular tilt, φ, or with the average distribution of the C(5) atom with respect to the molecular plane, which is equal to 1 for the low-temperature phase and 0 when the occupation of C(5) is 0.5 for two sites on opposite sides of the ring. These two parameters are interdependent, although the φ angle refers to the molecular orientation in the lattice and thus describes the displacements of atoms, while the order parameter based on the occupancy of C(5) is based on molecular conformation and reflects the order–disorder character of the transition. Two order parameters or a more complex form of the order parameter, involving both C(4) and C(5) atoms and their displacements, may be more appropriate for describing the continuous evolution of the DTA signal, H NMR M_2 second moment or the changes of permittivity (Waôsicki *et al.*, 1995) through T_c.

When the temperature of MCHD is raised, the difference between the Donohue angles of the $O(1)H\cdots O(2^i)$ hydrogen bond increases and stabilizes the H atom location at O(1) (see Fig. 9). Thus, a temperature-induced phase transition connected with hydrogen transfers is unlikely in this substance: the monotonous small changes of the hydrogen-bond dimensions reflect the continuous character of the phase transition in MCHD.

This study was supported by the Polish Committee of Scientific Research, partly by Project 2 P 30219304 and partly by Project 3 T09A 01511.

References

Barcon, A., Brunskill, A. P. J., Lalancette, R. A. & Thompson, H. W. (1998). *Acta Cryst.* C**54**, 1282–1285.
Baudour, J. L. (1996). *Cryst. Rev.* **5**, 227–264.
Bernstein, J. (1979). *Acta Cryst.* B**35**, 360–366.
Bernstein, J. & Hagler, A. T. (1978). *J. Am. Chem. Soc.* **100**, 673–681.
Błaszczyk, J., Wieczorek, M. & Okruszek, A. (1996). *J. Mol. Struct.* **374**, 85–96.
Braga, D. (1992). *Chem. Rev.* **92**, 633–665.
Byrn, S. R., Curtin, D. Y. & Paul, I. C. (1972). *J. Am. Chem. Soc.* **94**, 890–898.
Dunitz, J. D. (1995). *Acta Cryst.* B**51**, 619–631.
Eliel, E. L. & Wilen, S. H. (1994). *Stereochemistry of Organic Compounds.* New York: John Wiley and Sons, Inc.
Etter, M. C., Urbańczyk-Lipkowska, Z., Jahn, D. A. & Frye, J. S. (1986). *J. Am. Chem. Soc.* **108**, 5871–5876.
Facey, G. A., Connolly, T. J., Bensimon, C. & Durst, T. (1996). *Can. J. Chem.* **74**, 1844–1851.
Garbauskas, M. F., Goehner, R. P. & Davis, A. M. (1983). *Acta Cryst.* C**39**, 1684–1686.
Gdaniec, M., Milewska, M. J. & Połoński, T. (1999). *Angew. Chem. Int. Ed.* **38**, 392–395.
Głowiak, T. & Sobczak, J. M. (1992). *J. Crystallogr. Spectrosc. Res.* **22**, 673–678.
Hazen, R. M., Hoering, T. C. & Hofmeister, A. M. (1987). *J. Phys. Chem.* **91**, 5042–5045.
Herbstein, F. H. (1996). *J. Mol. Struct.* **374**, 111–128.
Johnson, C. K. (1965). *ORTEP*. Report ORNL-3794. Oak Ridge National Laboratory, Tennessee, USA.
Katrusiak, A. (1989). *Acta Cryst.* C**45**, 1897–1899.
Katrusiak, A. (1990). *Acta Cryst.* B**46**, 246–256.
Katrusiak, A. (1991). *Acta Cryst.* B**47**, 398–404.
Katrusiak, A. (1992). *J. Mol. Struct.* **269**, 329–354.
Katrusiak, A. (1993*a*). *Solid State Commun.* **86**, 87–91.
Katrusiak, A. (1993*b*). *J. Crystallogr. Spectrosc. Res.* **23**, 367–372.
Katrusiak, A. (1993*c*). *Phys. Rev. B*, **48**, 2992–3002.
Katrusiak, A. (1994). *Correlations, Transformations and Interactions in Organic Crystal Chemistry*, edited by D. W. Jones and A. Katrusiak, pp. 93–113. Oxford University Press.
Katrusiak, A. (1995*a*). *Crystallogr. Rev.* **5**, 133–180.
Katrusiak, A. (1995*b*). *Phys. Rev. B*, **51**, 589–592.
Katrusiak, A. (1996). *J. Mol. Struct.* **385**, 71–80.
Katrusiak, A. (1998). *Pol. J. Chem.* **72**, 449–459.
Katrusiak, A., Kałuski, Z., Pietrzak, P. & Skolik, J. (1983). *J. Crystallogr. Spectrosc. Res.* **13**, 151–163.
Konarski, J. (1984). *Wiadomości Chem.* **38**, 621–633.
Konno, M., Okamoto, T. & Shirotani, I. (1989). *Acta Cryst.* B**45**, 142–147.
Kroon-Batenburg, L. M. J., Bouma, B. & Kroon, J. (1996). *Macromolecules*, **29**, 5695–5699.
Kroon-Batenburg, L. M. J., Kroon, J. & Northolt, M. G. (1986). *Polym. Commun.* **27**, 290–292.
Lawalle, D. K. & Zeltman, A. H. (1974). *J. Am. Chem. Soc.* **96**, 5552–5556.
Le Bars-Combe, M. & Lajzerowicz, J. (1987). *Acta Cryst.* B**43**, 386–393.
Manz, J., Meyer, R., Pollak, E. & Romelt, J. (1982). *Chem. Phys. Lett.* **93**, 184–187.
Molchanov, V. N., Shibaeva, R. P., Kachinskii, V. N., Yagubski, E. B., Simonov, V. I. & Vainstein, B. K. (1986). *Sov. Phys. Dokl.* **286**, 637–640.
Näther, Ch., Nagel, N., Bock, H., Seitz, W. & Havlas, Z. (1996). *Acta Cryst.* B**52**, 697–706.
Ogawa, K., Kasahara, Y., Ohtani, Y. & Harada, J. (1998). *J. Am. Chem. Soc.* **120**, 7107–7108.
Ohashi, Y. (1998). *Crystalline-State Reactions of Cobaloxime Complexes.* Tokyo Institute of Technology, Tokyo.
Ono, H., Ishimaru, Sh., Ikeda, R. & Ishida, H. (1998). *Ber. Bunsenges. Phys. Chem.* **102**, 650–655.
Pająk, Z., Latanowicz, L. & Katrusiak, A. (1992). *Phys. Status Solidi A*, **130**, 421–428.
Parkinson, G. M., Thomas, J. M., Williams, J. O., Goringe, M. J. & Hobbs, L. W. (1976). *J. Chem. Soc. Perkin Trans.* **11**, 836–838.
Paul, I. C. & Go, K. T. (1969). *J. Chem. Soc. B*, pp. 33–42.
Richardson, M. R., Yang, Q., Novotny-Bregger, E. & Dunitz, J. D. (1990). *Acta Cryst.* B**46**, 653–660.
Rohleder, J. W. (1989). *Fizyka chemiczna kryształów molekularnych.* Państwowe Wydawnictwo Naukowe, Warsaw.
Rychlewska, U., Hodgson, D. J., Yeh, A. & Tien, H.-J. (1991). *J. Chin. Chem. Soc.* **38**, 467–473.
Semmingsen, D. A. (1974). *Acta Chem. Scand.* **28**, 169–174.

Sheldrick G. (1993). *SHELXL*93. University of Göttingen, Germany.
Thiel, J., Katrusiak, A. & Fiedorow, P. (2000). Submitted.
Thuery, P., Nierlich, M., Calemczuk, R., Saadioui, M., Asfari, Z. & Vicens, J. (1999). *Acta Cryst.* B**55**, 95–103.
Torrance, J. B., Vazques, J. E., Mayerle, J. J. & Lee, V. Y. (1981). *Phys. Rev. Lett.* **46**, 253–256.
Yalpani, M., Boese, R. & Bläser, D. (1983). *Chem. Ber.* **116**, 3338–3346.
Yalpani, M., Scheidt, W. R. & Seevogel, K. (1985). *J. Am. Chem. Soc.* **107**, 1684–1690.
Yang, Q., Richardson, M. R. & Dunitz, J. D. (1989). *Acta Cryst.* B**45**, 312–323.
VanDerveer, D. G. & Eisenberg, R. (1974). *J. Am. Chem. Soc.* **96**, 4994–4996.
Warshel, A. & Karplus, M. (1974). *J. Am. Chem. Soc.* **96**, 5677–5689.
Watenpaugh, K., Dow, J., Jensen, L. H. & Furberg, S. (1968). *Science*, **159**, 206–207.
Waôsicki, J., Czarnecki, P., Katrusiak, A., Ecolivet, C. & Bertault, M. (1995). *J. Phys. Condens. Matter*, **7**, 7489–7500.
Wysocka, W., Kolanoś, R., Borowiak, T. & Korzański, A. (1999). *J. Mol. Struct.* **474**, 207–214.